Reevaluation of T Cell Receptor Excision Circles as a Measure of Human Recent Thymic Emigrants[1]

Ping Ye and Denise E. Kirschner[2]

The human thymus exports newly generated T cells to the periphery. As no markers have been identified for these recent thymic emigrants (RTE), it is presently impossible to measure human thymic output. T cell receptor excision circles (TREC) have been recently used to assess thymic output during both health and disease. Using a mathematical model, we quantify age-dependent changes both in the number of RTE generated per day and in TREC concentration during an 80-year lifespan. Through analyses, we demonstrate that RTE and peripheral T cell division have the same potential to affect TREC concentration at any age in healthy people. T cell death also influences TREC concentration, but to a lesser extent. During aging, our results indicate that thymic involution primarily induces an age-dependent decline in TREC concentrations within both $CD4^+$ and $CD8^+$ T cell populations. We further apply this model for studying TREC concentration during HIV-1 infection. Our analyses reveal that a decrease in thymic output is the major contributor to the decline in TREC concentration within $CD4^+$ T cells, whereas both increased peripheral T cell division and decreased thymic output induce the decline in TREC concentration within $CD8^+$ T cells. Therefore, we suggest that T cell turnover should be examined together with TREC concentration as a measure of RTE. If peripheral T cell division remains relatively unchanged, then TREC concentration indeed reflects thymic output. *The Journal of Immunology,* 2002, 169: 4968–4979.**

The human thymus is the central lymphoid organ that provides a specialized microenvironment for maturation and selection for the majority of $\alpha\beta$ T lymphocytes. T cell generation through this thymic-dependent pathway is essential because it establishes and helps to maintain the peripheral T cell pool. This process also provides T cell repertoire diversity necessary for potential immune responses to a vast number of Ags (1). With increasing age, the lymphatic thymic mass decreases, and thymocyte production correspondingly declines (thymic involution) (2). Recent data suggest, however, that the adult thymus can remain active even late in life supplying functional T cells to the periphery (3, 4).

$CD4^+$ and $CD8^+$ T cells progress through several stages during their long lifespan. Both mature $CD4^+$ and $CD8^+$ thymocytes first emigrate from the thymus into the periphery as recent thymic emigrants (RTE).[3] After RTE further mature, they are classified as naive T cells that continually circulate through blood and lymphoid tissues. Measuring the number of RTE produced per day by the thymus allows for assessment of the thymic contribution to the peripheral T cell pool. It is especially important to monitor thymic production under conditions that influence T cell depletion and reconstitution, such as HIV-1 infection, bone marrow transplantation, and immunosuppressive therapy.

In chicken, mouse, and rat models, RTE have been identified using various markers. In chickens, $chT1^+$ T cells are classified as RTE, and the level of $chT1^+$ T cells has been shown to decline in parallel with thymic involution. These cells are distributed in peripheral blood and lymphoid tissues with a half-life of 3 days (5). In mice, FITC labeling of thymocytes and grafting of thymic lobes from congenic $Ly5.2^+$ mice have been used to study RTE (6, 7). Most mouse RTE survive in the periphery for 2–3 wk after release from the thymus. It is not clear whether these cells die or undergo further maturation. In rats, $Thy1^+CD45RC^-RT6^-$ are markers for RTE (8). These RTE were observed to differentiate into more mature T cells within 1 wk after emigrating from the thymus.

Due to the lack of phenotypic markers for RTE in humans, it is difficult to distinguish them from long-lived naive T cells (5, 9). Whether human RTE are fully functional or require maturation in the periphery needs further study. Therefore, direct quantification and characterization of RTE in humans are not yet possible. Currently, the term RTE in humans generally refers to T cells that have undergone only a few cellular divisions after leaving the thymus (10).

Recently, the concentration of T cell receptor excision circles (TREC) has been suggested as a measure for quantifying thymic output in humans (9, 10). During TCR gene rearrangement, excised DNA fragments are maintained in cells episomally as TREC. Two TREC species, signal-joint TREC (sjTREC) and coding-joint TREC (cj TREC), which are products of the deletion of the TCR δ locus from the TCR α locus during the first TCR α gene rearrangement, are produced sequentially by all $\alpha\beta$ T cells. In most of them, these TREC are generated without prior δ rearrangement and are hence identical and can be detected in ~70% of $\alpha\beta$ T cells (9). A maximum of two sjTREC and two cjTREC can be present within one $\alpha\beta$ T cell if the corresponding rearrangement event occurs in both alleles. TREC are exported from the thymus to the

[3] Abbreviations used in this paper: RTE, recent thymic emigrants; TREC, TCR excision circles; sjTREC, signal-joint TREC; cjTREC, coding-joint TREC; TN, $CD3^-CD4^-CD8^-$ triple-negative; ITTP, $CD3^-CD4^+CD8^-$ intrathymic T progenitor; DP, $CD3^+CD4^+CD8^+$ double-positive; SP4, $CD3^+CD4^+CD8^-$ single-positive; SP8, $CD3^+CD4^-CD8^+$ single positive; TES, thymic epithelial space; LT, lymphoid tissues; PRCC, partial rank correlation coefficients.

periphery within RTE. Thus, TREC levels in the periphery could reflect RTE numbers. TREC are stable and are not duplicated during mitosis; therefore, TREC concentration is diluted out with each cell division. This explains why thymocytes have higher TREC concentrations as compared with peripheral blood T cells (11, 12), and why naive T cells have higher TREC concentrations than memory T cells (10).

TREC concentration has been widely used as a measurement of the number of RTE during HIV-1 infection and treatment, hemopoietic stem cell transplantation, and thymectomy (9, 10, 13–16). However, controversy exists as to whether TREC concentrations are a good marker for RTE, because TREC concentrations are also affected by peripheral T cell turnover events, such as T cell division and death (9, 10, 17). Different techniques are used to measure TREC concentrations, such as real-time PCR (10, 17), quantitative-competitive-PCR (9, 13), and PCR-ELISA (18). Measurement units of TREC concentration vary as well, including TREC per 10^6 PBMCs (10), TREC per $CD45RA^+$ T cells (17), TREC per microgram DNA of T cells (9, 14), and TREC per 10^5 $CD4^+$ T cells (13). Together, these factors make it difficult to interpret and compare TREC data between studies.

It is not yet possible to experimentally differentiate the effects of thymic output and T cell turnover on TREC concentration in a quantitative way, because thymic output cannot be measured. To this end, we use mathematical modeling to predict whether TREC concentrations are a good marker of thymic function, as represented by the number of RTE. Our model captures age-dependent changes in thymopoiesis, RTE, and TREC levels. Using uncertainty and sensitivity analyses, we quantify the potential roles of thymic output, T cell division, T cell death, and intracellular TREC degradation in affecting TREC concentration at each specific age. We further define elements that contribute most to changes in TREC concentration that occur during aging and HIV-1 infection.

Human Thymopoiesis Model

To quantify age-dependent changes in thymic output per day (i.e., the number of RTE produced per day), we develop a model that describes human thymopoiesis. Bone marrow progenitor cells migrate to the thymus and differentiate into $CD3^-CD4^-CD8^-$ triple-negative (TN) cells. TN cells then differentiate into $CD3^-CD4^+CD8^-$ intrathymic T progenitor (ITTP) cells. ITTP cells give rise to the predominant thymocyte subset, $CD3^+CD4^+CD8^+$ double-positive (DP) cells. After positive and negative selection, the surviving DP cells further differentiate into either $CD3^+CD4^+CD8^-$ single-positive (SP4) or $CD3^+CD4^-CD8^+$ single-positive (SP8) cells (19). A minor subpopulation of both SP4 and SP8 cells emigrates to the periphery to become RTE and joins the T cell pool (19). Fig. 1 presents a diagram of this process. The equations and parameters for the human thymopoiesis model are discussed in the *Appendix*.

Quantification of human thymocytes and RTE

Once model equations are derived that describe Fig. 1 (see *Appendix*), we then solve the system numerically. We present graphs for the corresponding simulations of this virtual model of human thymopoiesis. To build the model, we require a representation for thymic epithelial space (TES), which is the functional thymic tissue containing all thymocytes. Fig. 2A shows data for the maximal number of thymocytes calculated from the volume of the TES region (solid dots) and our best fit function for these data (solid line) during an 80-year lifespan (see *Appendix*).

Using this function for TES region, we can simulate the model behavior presented in Fig. 1. Our model results suggest that five thymocyte subsets increase in numbers to a maximum value at age 1 year and then decrease at a rate of ~5% per year (Fig. 2B). When comparing curve shapes in Fig. 2A and Fig. 2B, it can be seen that age-dependent changes in the average number of thymocytes is proportional to the maximal number of thymocytes in the TES region. This implies that involution quantitatively affects thymopoiesis. Shown in Fig. 2C is the simulation for the average number of RTE produced per day during an 80-year lifespan for an individual. The numbers of $CD4^+$ and $CD8^+$ RTE produced per day increase to their greatest values at the age of 1 year and then decline with age. Total thymocyte number has a 2-log decrease

FIGURE 1. Model representing human thymopoiesis. Five thymocyte subsets are included, TN, ITTP, DP, SP4, and SP8 cells. Represented are thymocyte growth (γ_i) limited by the maximal number of thymocytes in thymic epithelial space ($T_{es}(t)$), thymocyte differentiation (f_j), death (d_i), and emigration to the periphery as RTE (e_1, e_2) ($i = 1, 2, 3, 4, 5$; $j = 1, 2, 3, 4$). The definitions and values of parameters are given in the *Appendix*.
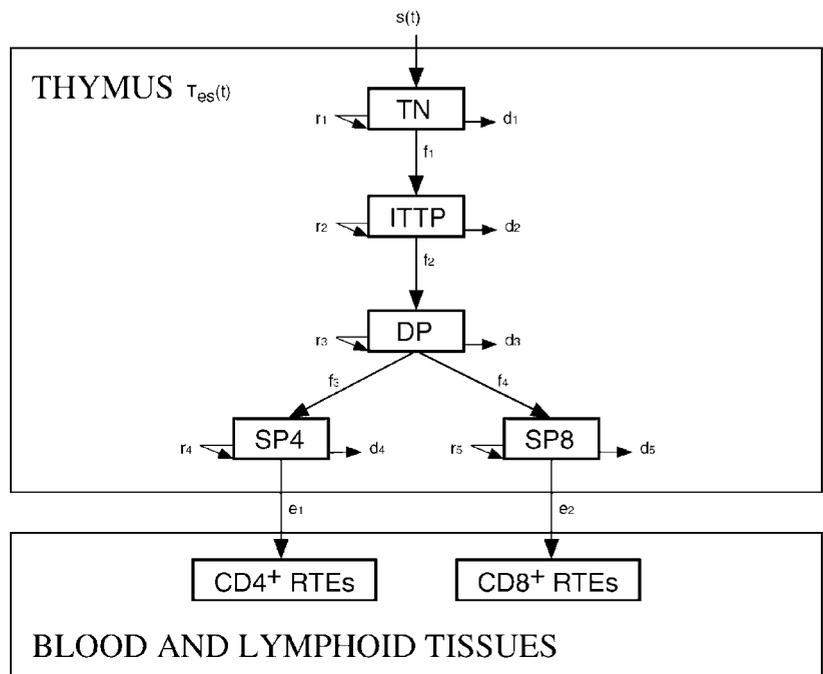
FIGURE 2. Thymopoiesis model illustrates thymic involution during 80 years of life. *A*, Best fit function ($T_{es}(t)$) (solid line) for data (●) derived from the volume of TES region (2). *B*, Model solutions of five thymocyte subsets. *C*, Number of RTE exported from the thymus per day. *D*, Total thymocytes (sum of five thymocyte subsets in *B*) and total RTE exported per day (sum of $CD4^+$ and $CD8^+$ RTE in *C*) on a log scale.
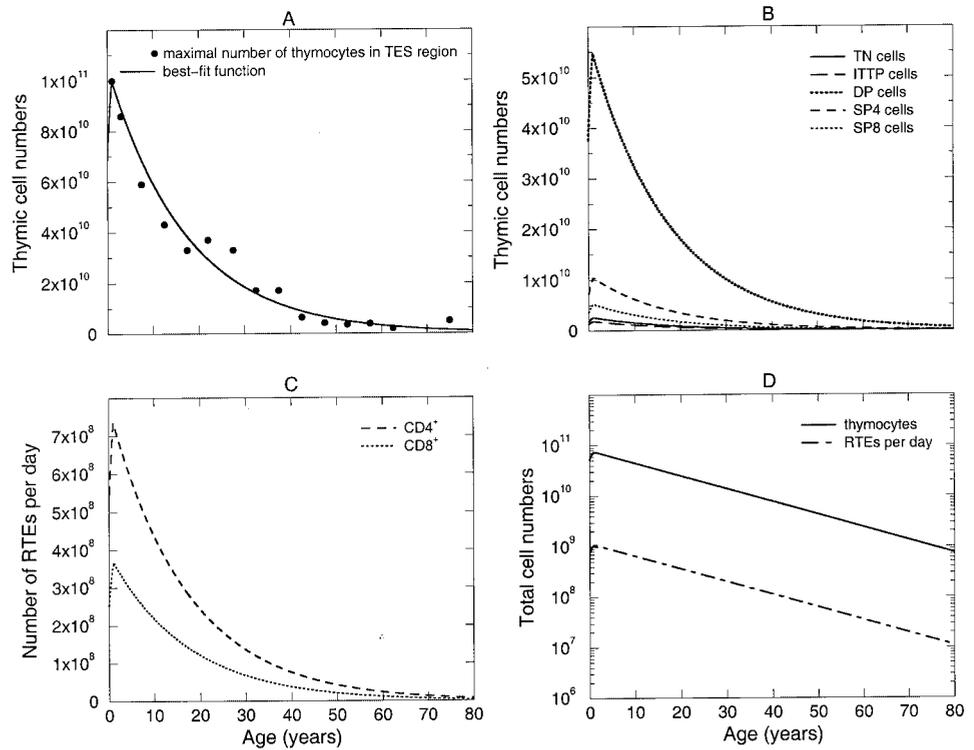
during 80 years. Correspondingly, the total number of RTE exported from the thymus per day declines exponentially by 2 orders of magnitude during 80 years (Fig. 2*D*).

The model predicts the observed ratio of SP4 to SP8 cells as 2, consistent with human data (19, 20). This ratio in the thymus determines the $CD4^+$:$CD8^+$ T cell ratio in the blood, which ranges from 1.5 to 2.5 (21). Our model predicts that the maximum number of thymic emigrants at the age of one is 1.1×10^9 cells/day (Fig. 2*D*), which is comparable with another estimate of human thymic emigrants of 10^9/day (22). Our virtual model also predicts that the ratio of thymic emigrants per day to total thymocyte numbers is 1.5%. This is consistent with experimental data ranging between 1 and 5% in mice (23). Thus, this model likely reflects the process of human thymopoiesis. More importantly, we quantify the number of RTE entering the periphery per day during the normal aging process, which cannot be measured experimentally (Fig. 2*C*).

Human TREC Model

The sjTREC concentration declines during aging and HIV-1 infection (9, 10, 17, 24). Some studies indicate that reduced thymic production of RTE contributes most to the decline of sjTREC concentration (9, 10, 24), whereas others suggest that increased cell division but not thymic dysfunction affects sjTREC concentration (17, 25). To address the question of whether the TREC concentration is mainly affected by thymic output or peripheral T cell turnover, we extended the thymopoiesis model to illustrate dynamic changes in sjTREC, the most ubiquitous human TREC species that is produced during TCR gene rearrangement, and the one that is most consistently measured experimentally. Fig. 3 presents the dynamics for sjTREC between the thymus and peripheral blood and lymphoid tissues (LT). Total T cell levels (including both naive and memory T cells) are influenced by thymic output of
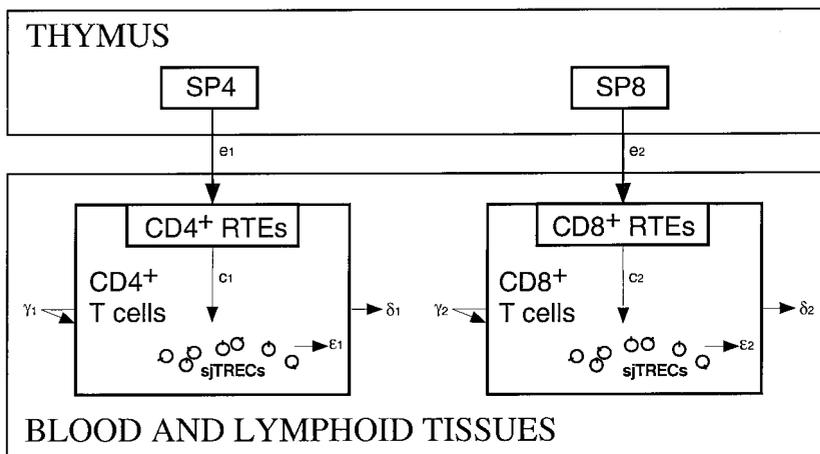
FIGURE 3. Model representing human sjTREC dynamics. Total sjTREC levels are affected by thymic output to the periphery as RTE (e_1, e_2), which contain sjTREC (sjTREC concentration within RTE c_1, c_2), T cell death (δ_1, δ_2), and sjTREC degradation (ϵ_1, ϵ_2). Total T cell levels are affected by thymic output of RTE (e_1, e_2), T cell growth (γ_1, γ_2), and T cell death (δ_1, δ_2). The sjTREC concentration within T cells is affected by each event. For simplicity, sjTREC in SP cells and RTE are not drawn. The definitions and values of parameters are given in the *Appendix*.

RTE, T cell growth, and T cell death. sjTREC are generated within thymocytes and exported to the periphery within RTE. Thus, total sjTREC levels are determined by thymic output of sjTREC, T cell death, and intracellular sjTREC degradation. Studies of sjTREC levels in thymectomized humans and macaques indicated that there is no significant extrathymic source of cells containing sjTREC (9, 11). T cell death induces the loss of sjTREC within T cells, and this loss of sjTREC is proportional to the loss of T cells. As the sjTREC concentration is determined by both total sjTREC levels and total T cell levels, events that affect them will indirectly induce changes in sjTREC concentration, including thymic output, T cell growth, T cell death, and sjTREC degradation. Using our TREC model, we reveal how thymic output and T cell turnover affect sjTREC concentrations at each specific age and during the entire lifespan in healthy people, and explore the principal factors contributing to the decline in sjTREC concentrations during HIV-1 infection. The equations and parameters for the human TREC model are discussed in the *Appendix*.

Predicting total T cell numbers, total sjTREC levels, and sjTREC concentration

The dynamic changes of $CD4^+$ and $CD8^+$ T cells in peripheral blood/LT based on our simulations are shown in Fig. 4A. The initial increase of T cells is due to the large output of newly generated T cells from the thymus in the early years of life (see Fig. 2C). Then, T cell numbers continuously increase until age 30 years. After age 30 years, T cell numbers remain at a relatively stable level with a slow decline over time, as suggested by data (26, 27). Our simulation results of T cell dynamics are within the normal range calculated from human data on cell numbers per mm^3 of blood, blood volume, and body weight (error bars in Fig. 4A) (26, 28–31). Increased peripheral T cell division maintains the 30-year increase and subsequent relative equilibrium in T cell numbers (data not shown). This is consistent with data from two animal models of older sooty mangabeys and mice that lack thymic function, indicating that most T cell production occurred in the periphery (27, 32).

Shown in Fig. 4B are changes in total sjTREC within both $CD4^+$ and $CD8^+$ T cells during 80 years. The level of total sjTREC in peripheral blood/LT reaches its maximum around 15 months of age and remains at that level for ~12 months. Then total sjTREC level decreases concomitant with the decline in number of RTE produced per day.

We simulate sjTREC concentration within $CD4^+$ T cells by dividing total levels of sjTREC within $CD4^+$ T cells with total $CD4^+$ T cells. In experimental measurements (9), results were presented in units of $sjTREC/1.5 \times 10^5$ T cells. Hence we multiply our sjTREC/T cell results by 1.5×10^5 (Fig. 4C, solid line). Similarly, we calculate the sjTREC concentration within $CD8^+$ T cells (Fig. 4D, solid line). The sjTREC concentrations for both $CD4^+$ and $CD8^+$ T cells decline ~2 logs during an 80-year period.

Douek et al. (9) reported that sjTREC concentrations decline by 1–1.5 logs in both blood $CD4^+$ and $CD8^+$ T cells during the lifetime of an individual (in units of $sjTREC/1.5 \times 10^5$ T cells). Zhang et al. (10) measured sjTREC level (α1 circles) per 10^6 PBMCs and found a total decrease of 2 logs over seven decades. To convert data from Ref. 10 into units of $sjTREC/1.5 \times 10^5$ T cells, we divide sjTREC/PBMCs with the ratios: total lymphocytes/PBMCs and T cells/total lymphocytes over time (26, 33, 34), and then multiply by 1.5×10^5 T cells. sjTREC data from Douek et al. and Zhang et al. were both measured using blood samples. The number of T cells in blood represents ~2% of total T cells in the body (35–37). We scale the data sets appropriately by assuming that T cells in humans continuously circulate between blood and lymph, exchanging in the blood 48 times daily in healthy individuals (35), and that the levels of sjTREC per T cell in blood are similar to sjTREC per T cell in LT. Our model results of average sjTREC concentrations in blood/LT during aging are comparable with two experimental data sets from Douek et al. and Zhang et al. (Fig. 4, C and D). The slight differences are likely due to different PCR techniques, target cell populations, and unit conversions used for data sets.

FIGURE 4. Model simulations during 80 years for levels of total T cells, total sjTREC, and sjTREC concentrations. A, Total T cells in peripheral blood/LT. The normal range for T cells is calculated from data on cell number/ mm^3 blood, blood volume and body weight (26, 28–31). B, Total sjTREC in peripheral blood/LT. C, sjTREC concentration within $CD4^+$ T cells (in units of $sjTREC/1.5 \times 10^5$ cells). D, sjTREC concentration within $CD8^+$ T cells (in units of $sjTREC/1.5 \times 10^5$ cells). The experimental data from Ref. 9 ($\triangle$) represent individual cases, whereas the data from Ref. 10 ($\blacktriangle$) are the median of multiple cases.
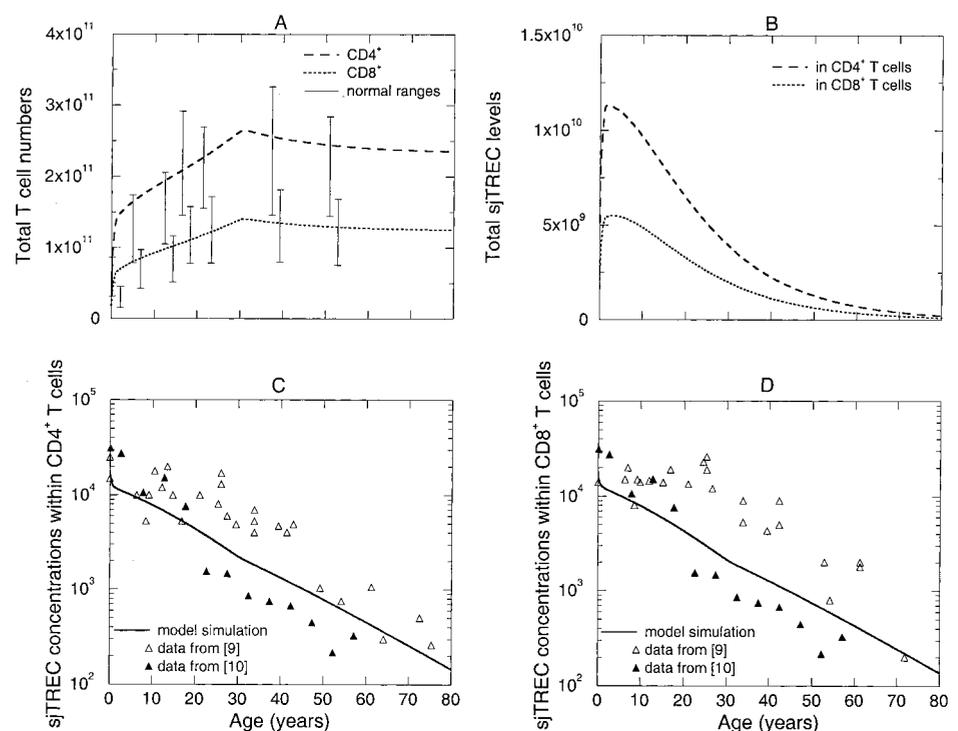
Elucidating principal factors contributing to TREC concentration in healthy people

The key to interpreting TREC data is to quantitatively distinguish between the effects of thymic output and T cell turnover on sjTREC concentration (38). Although T cell division and T cell death can be measured experimentally, RTE levels cannot. To explore how both thymic and peripheral events affect sjTREC concentration, we study the parameters that correspond to each of four events that determines the sjTREC concentration: thymic output; T cell division; T cell death; and sjTREC degradation. In this section, we address relative contributions of these four events to sjTREC concentration in healthy people, which will help interpret sjTREC data during T cell depletion conditions. To do this, we first examine how these four events affect sjTREC concentration at each specific age, and then we test how these four events combined induce sjTREC concentration decline during 80 years in healthy people.

sjTREC concentration dynamics at a given age. To address relative contributions to sjTREC concentration at a given age, we implement uncertainty and sensitivity analyses for four parameters: SP4 emigration rate; T cell division rate; T cell death rate; and sjTREC degradation rate (cf Ref. 39). Detailed methods for these analyses are discussed in the *Appendix*. We present results for one of the outcome variables, sjTREC concentration within $CD4^+$ T cells.

We first perform the uncertainty analysis by varying each parameter independently. Shown in Fig. 5 are the changes in sjTREC concentration in response to individual variations of each parameter. The solid line represents the median level of sjTREC concentration when the parameter is given its baseline value. The range between upper and lower bounds represents the 95% confidence interval for the simulated median of sjTREC concentration. According to the 95% confidence interval, thymic emigration, T cell division, and sjTREC degradation affect sjTREC concentration to a greater extent than does T cell death, and this is true at any age over 80 years of life ($p < 0.005$). No significant differences

FIGURE 6. Simulation of nine virtual sjTREC concentrations. This sensitivity analysis shows the effects of changing four parameters simultaneously that control thymic output, T cell division, T cell death, and sjTREC degradation on sjTREC concentration within $CD4^+$ T cells. Emigration rate of SP4 cells (e_1), T cell division rate (γ_1), T cell death rate (δ_1), and sjTREC degradation rate (ϵ_1) vary logarithmically 100-fold of baseline values. The unit for sjTREC concentration is sjTREC/1.5×10^5 cells.

are found between the effects of thymic output and T cell division ($p > 0.05$), and we assume the sjTREC half-life (degradation rate) is likely constant. Therefore, our results indicate that, at any age, when these events have similar magnitude changes, thymic output and peripheral T cell division can have an equal impact on sjTREC concentration, whereas T cell death affects it less.

We also perform the same uncertainty analyses for total sjTREC levels and total T cell levels. Our results indicate that decreased thymic output leads to a decrease in total sjTREC levels and total T cell levels, which is more evident early in life. Increased T cell division affects T cell levels, but not total sjTREC levels. Increased T cell death leads to a decrease in total sjTREC levels as well as T cell levels (data not shown).

The above experiments were performed by varying each of four events, thymic output, T cell division, T cell death, and sjTREC degradation, independently. What remains to be determined is the effect on sjTREC concentration when all four events are allowed to

FIGURE 5. Effects of independently altering thymic output or peripheral turnover events on sjTREC concentration within $CD4^+$ T cells. Model simulations of sjTREC median and 95% confidence interval provide the uncertainty in sjTREC concentration when varying one parameter at each time. Each parameter controls one of four events: thymic output; T cell division; T cell death; and sjTREC degradation. The unit for sjTREC concentration is sjTREC/1.5×10^5 cells. *A*, Changes in sjTREC concentration when varying emigration rate of SP4 cells (e_1) logarithmically from 0.007/day to 0.7/day. *B*, Changes in sjTREC concentration when varying T cell division rate (γ_1) logarithmically from 0.0002/day to 0.02/day. *C*, Changes in sjTREC concentration when varying T cell death rate (δ_1) logarithmically from 0.0002/day to 0.02/day. *D*, Changes in sjTREC concentration when varying sjTREC degradation rate (ϵ_1) logarithmically from 0.0002/day to 0.02/day.

Table I. *PRCC between sjTREC concentration and each parameter[a]*

Age (years)	SP4 Emigration Rate (e_1)	T Cell Division Rate (γ_1)	T Cell Death Rate (δ_1)	sjTREC Degradation Rate (ϵ_1)
5	0.73	−0.77	0.64	−0.86
10	0.74	−0.78	0.65	−0.84
20	0.76	−0.82	0.65	−0.86
40	0.82	−0.86	0.66	−0.84
70	0.84	−0.90	0.73	−0.86
Mean ± SD	0.78 ± 0.05*[†]	−0.82 ± 0.06*	0.67 ± 0.03	−0.85 ± 0.01*

[a] Parameter sensitivity is evaluated by PRCC. Data represent mean PRCC from 90 experiments, and each PRCC is significant at the 0.05 level.

*, $p < 0.005$, compared with T cell death rate using absolute values (Student's *t* test). †, $p > 0.05$, compared with T cell division rate using absolute values (Student's *t* test).

vary in combination. This sensitivity analysis will assess the importance of these four events relative to each other for inducing variability in sjTREC outcomes. Model simulations of sjTREC concentrations for nine virtual patients show large variations and different shape curves (Fig. 6) arising from uncertainties in the four governing parameters. Differences in the values of four parameters may explain the considerable discrepancy observed from patient to patient and study to study (Fig. 4, *C* and *D*) (9, 10, 24).

To explore which events contribute most to the variations observed in sjTREC concentration, we perform the same experiment 10 times (with 9 samples each time as in Fig. 6) by simultaneously varying all 4 parameters within a large range. Parameter sensitivity is represented by the mean partial rank correlation coefficients (PRCC) between sjTREC concentration and each parameter: emigration rate of SP4 cells; T cell division rate; T cell death rate; and sjTREC degradation rate, respectively. We perform this calculation at different ages to assess whether certain parameters have greater or lesser effects at different times (Table I). The SP4 emigration rate, T cell division rate, T cell death rate, and sjTREC degradation rate are all significantly correlated with sjTREC concentration at any age ($p < 0.05$). The contributions of thymic output, T cell division, and death to sjTREC concentration gradually increase during aging, whereas sjTREC degradation remains constant. Thymic output, T cell division, and sjTREC degradation are more critical in regulating sjTREC concentration than is T cell death ($p < 0.005$). No significant difference is observed between the effects of thymic output and T cell division on sjTREC concentration ($p > 0.05$). If we assume the half-life of sjTREC is relatively constant, our analyses suggest that both thymic output and T cell division can strongly and equally affect sjTREC concentration at any age. These results are consistent with our previous findings when varying the parameters individually (Fig. 5). Similar results are also observed for sjTREC concentration within CD8$^+$ T cells when varying these parameters (data not shown). This important finding distinguishes the relative roles of thymus and peripheral T cell turnover in regulating sjTREC concentration and provides a quantitative rule to characterize which events affect sjTREC concentration during disease states.

sjTREC concentration dynamics during 80 years. The uncertainty and sensitivity analyses characterized how thymus and T cell events can affect sjTREC concentration at each specific age. To assess the sjTREC concentration decline during the overall aging process, we simulate the sjTREC concentration within CD4$^+$ T cells using either a constant thymic output, or a constant growth rate, or a constant death rate (values at age 1 year). As shown in Fig. 7, when fixing either the growth rate (dashed line) or the death rate (long dashed line) to be constant, simulations of sjTREC concentration have a similar trend of decline as the healthy controls (solid line). However, when thymic output is maintained at a fixed

level, the resulting simulation of sjTREC concentration remains in a relatively steady state during 80 years (dotted line). This finding indicates that decreased output of RTE due to thymic involution predominantly elicits the decline of sjTREC concentration within CD4$^+$ T cells during aging. This result is robust when we apply any constant values for thymic output, T cell growth rate, or T cell death rate (data not shown). Similar results are achieved for sjTREC concentration within CD8$^+$ T cells (data not shown). Therefore, sjTREC concentration can represent thymic output for healthy people during the aging process.

Elucidating principal factors contributing to TREC concentration decline during HIV-1 infection

Our human thymopoiesis and TREC model provides a systematic way to quantitatively analyze how the thymus and peripheral T cell turnover contribute to changes in sjTREC concentration during T cell depletion situations, such as HIV-1 infection, hemopoietic stem cell transplantation preceded by chemoradiotherapy, thymectomy, and chemotherapy.

To apply our TREC model as a predictor of thymic function, we examine an HIV-1 infection scenario. HIV-1 disease is characterized by a gradual decline of CD4$^+$ T cells, with an initial rise followed by a fall in CD8$^+$ T cells during a 10-year period typically (40). sjTREC concentrations within both CD4$^+$ and CD8$^+$ T cells decrease during early HIV-1 infection (9, 13). Some studies suggest that the decline in sjTREC concentration results from a decrease in thymic output (9, 41). Evidence shows that HIV-1
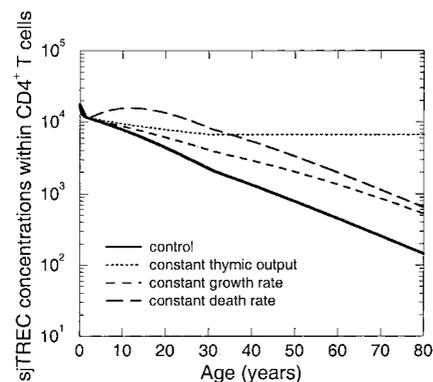
FIGURE 7. Simulation of sjTREC concentration within CD4$^+$ T cells during aging. The solid line represents simulation of healthy controls. The dotted line represents simulation using the thymic output at age 1 as the constant thymic output during 80 years. The dashed line represents simulation using the growth rate at age 1 year as the constant growth rate during 80 years. The long dashed line represents simulation using the death rate at age 1 year as the constant death rate during 80 years.

interrupts thymopoiesis by directly infecting CD4^{+} thymocytes and stromal cells, inducing the decline of thymic output (42, 43, 44). Other studies indicate that global immune activation induced by HIV-1 leads to increased cell division, causing the dilution of sjTREC concentration (17, 25).

Experimental studies suggest that the division rate of CD4^{+} T cells in patients with HIV-1 infection increases ~1- to 2-fold as compared with uninfected controls, whereas the division rate for CD8^{+} T cells increases 7- to 8-fold as compared with uninfected controls (25, 45, 46, 47). Death rates of both CD4^{+} and CD8^{+} T cells increase 3- to 4-fold during HIV-1 infection (45, 46). No quantitative data have been reported as to how RTE levels change during HIV-1 infection, due to the lack of a phenotypic marker for human RTE. This is the basic question that hinders distinguishing the relative role of the thymus in HIV-1 infection. However, our model provides a method to address this question.

As shown in Fig. 8, we simulate changes in sjTREC concentrations and T cell levels during early HIV-1 infection in a virtual group of people age 30 years. To achieve dynamics similar to those reported by clinical data for both T cells and sjTREC concentrations, our model predicts that thymic output of CD4^{+} RTEs must decline 10- to 15-fold, and thymic output of CD8^{+} RTEs must decline 1- to 6-fold. Experimental data show that HIV-1 directly infects CD4^{+} thymocytes and causes the SP4:SP8 ratio to invert from 2 to 0.5 (20, 42), suggesting that the decrease in CD4^{+} RTE is greater than that occurring in CD8^{+} RTE, which is consistent with our model predictions.

Our analyses reveal that although sjTREC concentrations within CD4^{+} and CD8^{+} T cells similarly decline during HIV-1 infection, factors that contribute to these phenomena differ according to changes in kinetics of thymic output predicted by our model and T cell turnover reported from literature. Because similar level changes in thymic output and T cell division elicit parallel changes in sjTREC concentration and similar level changes in T cell death induce much less of an effect to sjTREC concentration for a short period of time, our results suggest that decreased thymic output

mainly induces the decline of CD4^{+} sjTREC concentration, whereas increased peripheral T cell division and decreased thymic output both contribute to the decline in CD8^{+} sjTREC concentration. Therefore, sjTREC concentration within CD4^{+} T cells is an adequate representation of RTE levels; however, sjTREC concentration within CD8^{+} T cells is not a useful representation of thymic output during HIV-1 infection.

Discussion

The number of RTE exported from the thymus per day is a critical representation of thymic function. This is particularly important for reconstitution of the immune system under conditions resulting in temporary or permanent T cell depletion. Measuring the number of RTE produced per day is an invaluable tool for studying establishment of the naive T cell repertoire, as well as for providing age-dependent changes in thymic contribution to the peripheral T cell pool under normal conditions.

Characterization of human RTE has been hampered by the lack of a marker that distinguishes them from long-lived naive T cells. A number of phenotypic markers have been used for the evaluation of naive T cells, with no clear understanding of which naive phenotype is best enriched for by RTE, including CD45RA^{+} CD45RO^{−}, CD45RA^{+}CD62L^{+}, CD45RO^{−}CD27^{+}CD95^{low} (48). One study using a phenotypic approach suggested that CD103-bearing naive CD8^{+} T cells are a subpopulation of human RTE (12). Another study indicated that cord blood naive T cells are human RTE (49). These identified RTE have rapid rates of apoptosis like thymocytes, and the presence of IL-7 maintains their survival and expansion in an Ag-independent manner.

Our first objective was to quantify age-dependent changes in total numbers of human RTE produced per day, which cannot be experimentally measured. We develop a model of human thymopoiesis to capture thymic involution. This is the first model for studying human thymopoiesis and quantifying the number of RTE exported per day, and our model is developed based mainly on

FIGURE 8. Simulation of changes in T cell levels and sjTREC concentrations during early HIV-1 infection in a virtual group age 30 years. The solid line represents simulation of healthy controls. The dotted line and error bars represent simulation of means and 95% confidence intervals of means, respectively, for HIV-1-infected people. For CD4^{+} cells, thymic output is decreased 10- to 15-fold, cell division is increased 1- to 2-fold, and cell death is increased 3- to 4-fold, as compared with healthy controls. For CD8^{+} cells, thymic output is decreased 1- to 6-fold, cell division is increased 7- to 8-fold, and cell death is increased 3- to 4-fold, as compared with healthy controls. The unit for sjTREC concentration is sjTREC/1.5 × 10^{5} cells. *A*, Changes in CD4^{+} T cells. *B*, Changes in CD8^{+} T cells. *C*, Changes in sjTREC concentration within CD4^{+} T cells. *D*, Changes in sjTREC concentration within CD8^{+} T cells.
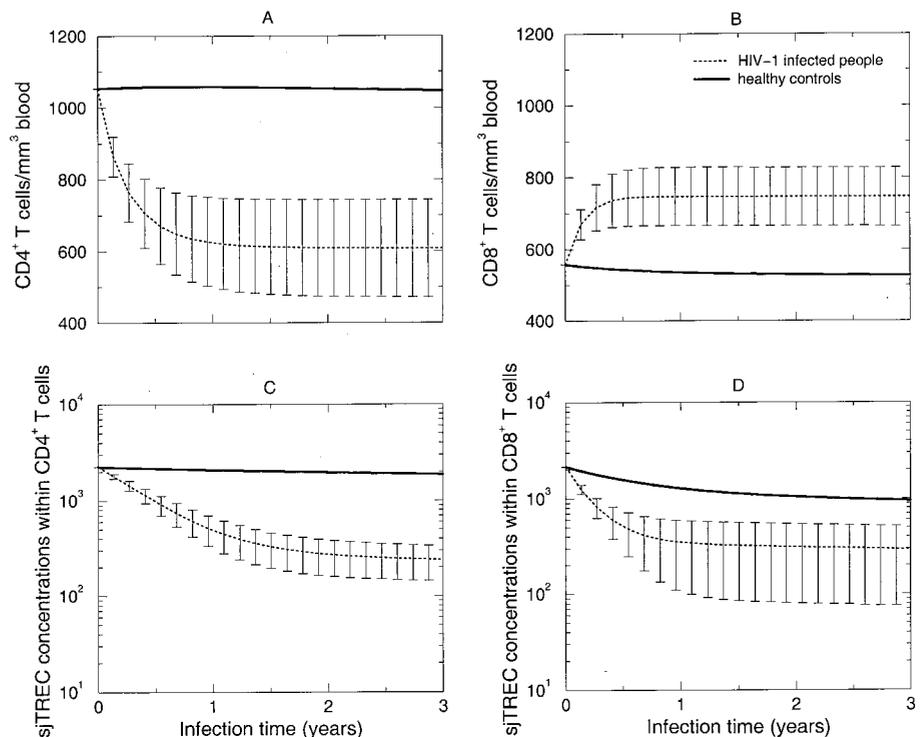
human experimental studies. Our results indicate that thymic output per day decreases exponentially by two orders of magnitude during 80 years (Fig. 2D). These are useful data for monitoring thymic function in healthy individuals, as well as providing a baseline comparison of thymic output during disease states.

We quantify thymic output as a rate measurement of the number of RTE produced per day. Currently, the longevity and migration patterns of human RTE are not known, rendering the calculation of total numbers of RTE in the peripheral blood/LT difficult. However, total RTE levels are mainly affected by thymic output per day. Thus, monitoring thymic output per day is a more direct and accurate estimation of thymic function as compared with total RTE numbers.

Recently, TREC concentration has been widely used to measure thymic output. Data suggest that TREC levels change during aging and disease (9, 10, 13, 14, 15, 17, 24, 41). However, it is still an open question as to whether TREC concentrations are mainly affected by thymic output or peripheral T cell events. Different techniques have been used to measure TREC levels, and the unit for measuring TREC levels varies from study to study, which can affect interpretation of TREC data (9, 10, 17, 18).

Our second aim was to verify whether TREC concentration is an accurate predictor of thymic function, represented by the number of RTE produced per day during aging and HIV-1 infection. We first simulate sjTREC concentrations as they change with age and validate our model with two experiment data sets. Using uncertainty and sensitivity analyses, we next quantify how key processes potentially control the dynamics of sjTREC concentration. Our results strongly suggest that thymic output and peripheral T cell division could equally affect sjTREC concentration at any age. T cell death contributes less to changes in sjTREC concentration than do thymic output and T cell division. We further demonstrate that sjTREC concentration is a good measurement for both CD4$^+$ and CD8$^+$ RTE in healthy people and for CD4$^+$ RTE during HIV-1 infection. Our findings have implications for interpreting TREC data during other T cell depletion situations, such as hemopoietic stem cell transplantation, thymectomy, and chemotherapy. We propose that peripheral T cell division and death should be examined before considering TREC concentration as a representation of thymic function.

A previous modeling study (17) suggested that only T cell division determines changes in TREC concentrations during aging and HIV-1 infection. This result is based on the assumption that neither division of naive T cells nor intracellular degradation of TREC occurs. Although division rates of naive cells are relatively low, they are unlikely to be zero. Their results later show that naive T cell division does occur. Similarly, although TREC are stably maintained within T cells, they have a finite half-life, likely shorter than or close to the half-life of T cells; TREC in chickens have been shown to have a half-life of ~2 wk (50). Our model predicts that sjTREC degradation rate is 0.002/day, similar to the T cell death rate, for example. The previous study (17) further assumes that naive T cell numbers are proportional to thymic output, and thus TREC concentration is not a measurement of thymic output but of T cell division. However, data suggest that naive T cell numbers and thymic output are not proportional, given that a subset of naive T cells have a very long lifespan and a subset of memory T cells can revert back to naive phenotype (22).

Recent clinical data support the thymus as a key contributor to TREC concentration decline during aging and HIV-1 infection (38, 41). One study suggests that changes in peripheral T cell division do not adequately explain many observations of TREC concentrations, including similar ratios of CD4$^+$ TREC to CD8$^+$ TREC in HIV-1-infected patients and healthy controls, similar TREC responses for discordant responders and good responders to antiret-

roviral therapy, and increased TREC concentration despite increased proliferation of T cells immediately after antiretroviral therapy (41). Another study indicates that the TREC concentration indeed reflects thymic output during aging (38). This study further suggests that thymic output most likely affects TREC concentration within CD4$^+$ T cells and that a combination of increased T cell division and decreased thymic output reduces TREC concentration within CD8$^+$ T cells after HIV-1 infection (38). These results are consistent with our model predications for TREC concentrations during both aging and HIV-1 infection scenarios.

Almost all TREC studies in humans are performed using peripheral blood. However, the majority of T cells (~98%) exist in the peripheral lymphoid system (35–37). Thus, quantification of TREC levels in different LT compartments would contribute greatly to our understanding of TREC dynamics. One study using a primate animal model observed that CD4$^+$ and CD8$^+$ T cells present in the lymph nodes contain more sjTREC than do peripheral blood T cells, suggesting that RTE can home into lymphoid tissues (11). Another study using a rat model observed that the percentages of RTE among T cell population were comparable in blood and all other LT compartments, indicating that rat RTE continuously migrate through blood and lymphoid organs as naive T cells (51). Our TREC model presents average sjTREC concentrations in peripheral blood/LT assuming that the sjTREC concentration in T cells within LT is similar to those in peripheral blood T cells. If the results from the primate animal model is applicable to humans, then our model simulations of the sjTREC concentration represent a lower boundary approximation.

Quantification of TREC concentration in two distinct pools of memory and naive T cells is an important next step. TREC concentration has been measured in the naive T cell pool (17). The differences in turnover rates of these T cell subclasses can further elucidate TREC dynamics. Currently, most experiments on TREC concentration are measured using CD4$^+$ and CD8$^+$ T cells (9, 11–13, 18, 38, 41, 48). Therefore, we can accurately build a model for TREC dynamics in these two compartments. Our model can be further adapted to explore TREC dynamics in memory and naive T cell pools when more data are available.

Overall, this study characterizes the relative roles of thymic output and periphery T cell turnover in regulating TREC concentrations. We propose that peripheral T cell division and death should be examined together with TREC concentration. Our model can be used as an integrated system for testing whether TREC concentration is an accurate marker for RTE levels in all situations by incorporating both T cell dynamics and TREC concentrations that are experimentally measured.

Appendix
Human thymopoiesis model

Defining mathematical notation for the terms shown in Fig. 1, $T(t)$ represents TN cells at time t, $I(t)$ represents ITTP cells, $D(t)$ represents DP cells, $S_4(t)$ represents SP4 cells and $S_8(t)$ represents SP8 cells. The mathematical representation describing the interaction of these five thymocyte subsets is based on a previous model of mouse thymocyte subsets (52). However, the thymopoiesis process is different in humans and mice (compare Refs. 19 and 23), and our model reflects these differences. We suppress the time dependence, (t), in the variables for ease of readability, except where needed for emphasis:

$$\frac{dT}{dt} = s(t) + r_1\left(1 - \frac{z(t)}{T_{es}(t)}\right)T - f_1 T - d_1 T, \qquad (1)$$

$$\frac{dI}{dt} = f_1 T + r_2\left(1 - \frac{z(t)}{T_{es}(t)}\right)I - f_2 I - d_2 I, \qquad (2)$$

$$\frac{dD}{dt} = f_2 I + r_3\left(1 - \frac{z(t)}{T_{es}(t)}\right)D - f_3 D - f_4 D - d_3 D, \qquad (3)$$

$$\frac{dS_4}{dt} = f_3 D + r_4\left(1 - \frac{z(t)}{T_{es}(t)}\right)S_4 - e_1 S_4 - d_4 S_4 ,\qquad(4)$$

$$\frac{dS_8}{dt} = f_4 D + r_5\left(1 - \frac{z(t)}{T_{es}(t)}\right)S_8 - e_2 S_8 - d_5 S_8 .\qquad(5)$$

Equations 1–5 describe a model of human thymopoiesis. The proliferation of thymocyte subsets, namely TN, ITTP, DP, SP4, and SP8, is logistically limited by the maximal number of thymocytes in TES region $T_{es}(t)$ for the sum of five thymocyte subsets $z(t)$. Each subset has a gain term from the previous cell stage, a differentiation term to the next stage of maturation, and a death term. In Equations 4 and 5, $e_1 S_4$ and $e_2 S_8$ represent the number of RTE that joins the peripheral T cell pool per day. By calculating the value of these two terms, our model provides a way to quantify RTE levels, which are not experimentally measurable in humans.

Human TREC model

TREC concentrations are determined by total TREC dynamics and total T cell dynamics. Define T_4 and T_8 to represent total CD4$^+$ and CD8$^+$ T cells in both blood/LT, respectively, and τ_4 and τ_8 to represent total sjTREC levels within CD4$^+$ and CD8$^+$ T cells in both blood/LT, respectively. Then a model for sjTREC and T cell dynamics based on Fig. 3 is given by

$$\frac{dT_4}{dt} = e_1 S_4 + \gamma_1\frac{k_4(t)T_4}{T_4 + s_1} - \delta_1\frac{T_4}{k_4(t)}T_4 ,\qquad(6)$$

$$\frac{dT_8}{dt} = e_2 S_8 + \gamma_2\frac{k_8(t)T_8}{T_8 + s_2} - \delta_2\frac{T_8}{k_8(t)}T_8 ,\qquad(7)$$

$$\frac{d\tau_4}{dt} = c_1 e_1 S_4 - \delta_1\frac{T_4}{k_4(t)}\tau_4 - \epsilon_1\tau_4 ,\qquad(8)$$

$$\frac{d\tau_8}{dt} = c_2 e_2 S_8 - \delta_2\frac{T_8}{k_8(t)}\tau_8 - \epsilon_2\tau_8 .\qquad(9)$$

The thymus provides newly generated T cells to the periphery ($e_1 S_4$, $e_2 S_8$), and the level of thymic output gradually declines during aging. Regenerative division of T cells ($\gamma_1\,[k_4(t)T_4/(T_4 + S_1)]$, $\gamma_2\,[k_8(t)T_8/(T_8 + S_2)]$) helps to maintain peripheral T cell homeostasis during human growth, as a compensation to the involution of thymic function (27, 32). Death of T cells ($\delta_1\,[T_4/k_4(t)]T_4$, $\delta_2\,[T_8/k_8(t)]T_8$) occurs in a density-dependent fashion. In division and death terms, $k_4(t)$ and $k_8(t)$ represent the average numbers of total CD4$^+$ and total CD8$^+$ T cells in the peripheral blood/LT, respectively. Here we model T cell dynamics for healthy individuals during ag-

ing; thus T cell growth and death are not further induced by Ag and inflammatory signals.

Total sjTREC levels are mainly affected by three processes: input from the thymus ($c_1 e_1 S_4$, $c_2 e_2 S_8$), loss due to death of T cells ($\delta_1\,[T_4/k_4(t)]\tau_4$, $\delta_2[T_8/k_8(t)]\tau_8$), and loss due to degradation of sjTREC within T cells ($\epsilon_1\tau_4$, $\epsilon_2\tau_8$). The loss of TREC due to T cell death is proportional to T cell death. We do not include T cell division and differentiation terms, because these two processes do not affect total sjTREC levels. With dynamics of both total sjTREC and total T cells, TREC concentrations can be simulated by dividing sjTREC by T cells.

Parameter estimation

The variables and parameters used in the human thymopoiesis model Equations 1–5 are defined in Table II. The parameters are the rate coefficients for each process described. Values for variables and rates were estimated from the literature. We give weight to human data, followed by data generated by murine and in vitro systems. For rates for which poor or no data exist, we perform uncertainty and sensitivity analyses to explore the change in outcomes over a full range of possible values. We outline below how we estimated the parameters.

Although the thymus undergoes involution during aging, the distribution of thymocyte subsets that is seen in adults is similar to the distribution observed in fetuses (3). TREC levels per thymocyte in adults also appear to be the same in fetuses and newborns (3). Thymic stromal cells, which are associated with thymocyte development, remain present and active throughout life (53). These data suggest that the effect of aging on the thymus appears to be quantitative rather than qualitative. To describe thymic involution dynamics, we represent the maximal number of thymocytes in TES region, $T_{es}(t)$, and the bone marrow cell source, $s(t)$, as time-dependent functions:

$$T_{es}(t)$$
$$= \begin{cases} 4.20 \times 10^{12} \times (0.002825e^{-0.001481t} + 0.001358) \times w(t) & \text{for } 0 \le t \le 1 \text{ year} \\ T_{es}(1\text{ yr}) \times 0.943^{\frac{t-365}{365}} & \text{for } 1 \text{ year} < t \end{cases}$$
$$\qquad(10)$$

$$s(t) = \frac{5 \times 10^8}{10^{11}}T_{es}(t)\qquad(11)$$

where $w(t) = 3.911 + 4.082(t/365) - 0.060(t/365)^2$ is the function for body weight. The body weight function is obtained by fitting data (28) using nonlinear least squares.

The lymphatic thymic tissue is composed of TES and perivascular space (2). The TES region, where thymopoiesis occurs, contains all of

Table II. *Variables and parameters defined in the thymopoiesis model*

Variable	Definition	Value[a]	Unit	References
T	TN cells	1.80×10^9	/thymus	3, 19, 58
I	ITTP cells	1.29×10^9	/thymus	3, 19, 58
D	DP cells	3.76×10^{10}	/thymus	3, 19, 58
S_4	SP4 cells	7.21×10^9	/thymus	3, 19, 58
S_8	SP8 cells	3.61×10^9	/thymus	3, 19, 58
Parameter				
r_1	Growth rate of TN cells	1.5	/day	23
r_2	Growth rate of ITTP cells	1.0	/day	23
r_3	Growth rate of DP cells	1.5	/day	23
r_4	Growth rate of SP4 cells	0.5	/day	23
r_5	Growth rate of SP8 cells	0.5	/day	23
f_1	Differentiation rate of TN cells into ITTP cells	0.3	/day	19
f_2	Differentiation rate of ITTP cells into DP cells	0.5	/day	19
f_3	Differentiation rate of DP cells into SP4 cells	0.04	/day	3, 59
f_4	Differentiation rate of DP cells into SP8 cells	0.02	/day	3, 59
e_1	Emigration rate of SP4 cells	0.07	/day	7
e_2	Emigration rate of SP8 cells	0.07	/day	7
d_1	Death rate of TN cells	0.27	/day	23, estimated
d_2	Death rate of ITTP cells	0.17	/day	23, estimated
d_3	Death rate of DP cells	0.33	/day	23, estimated
d_4	Death rate of SP4 cells	0.26	/day	23, estimated
d_5	Death rate of SP8 cells	0.26	/day	23, estimated

[a] Values for variables are initial values.

the thymocytes. A precise correlation has been shown between the number of RTE and functional thymic tissue in chickens (5). Here we assume that the volume of the TES region represents the maximum allowable number of thymocytes, i.e., the carrying capacity of the thymus for total thymocytes. The TES region reaches its highest level of 21.8 cm³ by the age of one (2), containing maximally 10^{11} thymocytes (54). We use the ratio 10^{11} thymocytes/21.8 cm³ TES volume to calculate the maximal number of thymocytes from the TES volume (Fig. 2A). The values for the TES volume are obtained by subtracting the mean volume of perivascular space from the mean volume of lymphatic thymic tissue by corresponding age groups from a stereological evaluation of 136 human thymuses (2). The maximal number of thymocytes, $T_{es}(t)$, can be obtained by a best fit function using nonlinear least squares (Equation 10 for 1 year < t). The thymic involution rate is 5.66% per year after the first year of life. During the first year of life, the function defining the maximal number of thymocytes is derived from the calculation of thymus weight (Equation 10 for $0 \leq t \leq 1$ year) (55).

Bone marrow shows no loss of function with age (54); however, the recovery of normal T cell subsets after bone marrow transplantation depends on thymic function (56, 57). On the basis of this evidence, we assume that the number of source cells from bone marrow utilized by the ethymus is determined by the number of available thymocytes. Thus, we track this change in cell source, $s(t)$ (Equation 11), as a function of $T_{es}(t)$. The seeding rate of progenitor cells into TN cells is 5×10^4 per day in young mice (23). Because the human thymus is 3 to 4 orders of magnitude larger than the mouse thymus, 5×10^8 per day is used as the cell source for TN cells at age 1 year.

The initial value of total thymocytes is 75% of maximal number of thymocytes, implying that one-third of total thymocytes are produced each day. This is derived from a calculation of growth rates, which is consistent with experimental reports (23, 58). The percentages of TN, ITTP, DP, SP4, and SP8 cells are 3.5, 2.5, 73, 14, and 7%, respectively, from studies of human thymic specimens (3, 19). Thus, the initial values for the five thymocyte subsets are calculated by multiplying 75% of maximal number of thymocytes at birth by the corresponding subset percentage. This allows for up to a 25% increase in thymocyte number.

Growth rates of thymocytes have been measured experimentally in the range of 0.5–1.5/day in mice (23). Generally, immature thymocytes have greater potential for expansion, whereas mature SP cells grow relatively slowly (23). We estimate growth rates of TN, ITTP, DP, SP4, and SP8 cells to be 1.5/day, 1.0/day, 1.5/day, 0.5/day, and 0.5/day, respectively.

It takes 3 days on average for TN cells to differentiate into ITTP cells (19); thus, the differentiation rate for TN cells is 0.3/day. Similarly, the differentiation rate for ITTP cells is calculated as 0.5/day (19). Approximately 5% of DP cells survive positive and negative selection to become SP cells (59), and the ratio of SP4/SP8 equals 2 (3); therefore, we estimate the differentiation rates of SP4 and SP8 cells to be 0.04/day and 0.02/day, respectively. Newly formed SP cells spend an average of 14 days in the thymus before emigration into the periphery as observed in a murine thymus system (7). Hence emigration rates of SP4 and SP8 cells are estimated as 0.07/day.

Although no available data exist for death rates of subsets of human thymocytes, the average lifespan of mouse thymocytes has been estimated to be 3 days (23). If we assume that the thymus is in steady state over a

short time, then the maximal number of thymocytes and cell source are constant and Equations 1–5 can be set to 0 (i.e., no change in the cell rates). Based on that assumption, the death rates for the five subsets of thymocytes can be calculated to be 0.27/day, 0.17/day, 0.33/day, 0.26/day, and 0.26/day, for TN, ITTP, DP, SP4, and SP8 cells, respectively.

The variables and parameters used in the human TREC model Equations 6–9 are defined in Table III. The average numbers of CD4⁺ and CD8⁺ T cells in the blood linearly increase during the first 30 years of life and then reach a relative steady state, considering age-dependent changes in cell number per mm³ blood, blood volume, and body weight (26, 28–31). We assume that the number of T cells in the LT have a pattern similar to that in the blood during human growth. Thus, the functions for the average numbers of total CD4⁺ and total CD8⁺ T cells in the peripheral blood/LT are as follows:

$$k_4(t) = \begin{cases} 6.5 \times 10^9 \times \dfrac{t}{365} + 4.33 \times 10^{10} & \text{for } 0 \leq t \leq 30 \text{ years} \\ k_4(30 \text{ yr}) & \text{for } 30 \text{ years} < t \end{cases}$$
(12)

$$k_8(t) = \begin{cases} 3.7 \times 10^9 \times \dfrac{t}{365} + 1.80 \times 10^{10} & \text{for } 0 \leq t \leq 30 \text{ years} \\ k_8(30 \text{ years}) & \text{for } 30 \text{ yr} < t \end{cases}$$
(13)

Conflicting data exist regarding the lifespan of T cells. The half-life of T cell subgroups are likely different as well. For example, naive T cells may live longer than memory T cells (45, 46). Literature suggests that the T cell death rate ranges from 0.00014/day to 0.014/day (45, 46, 60). Because the death rate in this model is the average death rate for the total CD4⁺ T cell population or for the total CD8⁺ T cell population, and the half-life for CD4⁺ and CD8⁺ T cells is similar (45, 46), we choose the value 0.002/day for both death rates of CD4⁺ and CD8⁺ T cell populations, respectively. Similarly, the division rate of T cells has been estimated within the range of 0.00078/day to 0.01/day (45, 60). We choose the value 0.002/day for both CD4⁺ and CD8⁺ T cell division rates. Half-saturation constants s_1 and s_2 are estimated from the model simulation as 10^{10}.

There were approximately 200,000 cjTREC per 150,000 CD4⁺ and CD8⁺ T cells (100% naive type) observed in cord blood (9). Three to four cell divisions occur between rearrangements that produce sjTREC and cjTREC (9). Thus, on average $200,000/2^{3.5} = 17677.67$ sjTREC exist within 150,000 CD4⁺ and CD8⁺ T cells in cord blood. The concentration of sjTREC within cord blood T cells is calculated to be $17677.67/150,000 = 0.118$/cell. The sjTREC concentration in cord blood CD4⁺ T cells is similar to that in CD8⁺ T cells (9). Another study observed that cord blood T cells have high levels of TREC compared with adult naive T cells, indicating that cord blood T cells do represent RTE (49). Thus, we use 0.118 sjTREC/cell for concentrations of sjTREC within CD4⁺ and CD8⁺ RTE.

The degradation rate of TREC in chickens is 0.05/day, calculated from a half-life of 2 wk (50). It is not known how long it takes for sjTREC to degrade in human T cells. We hypothesize that degradation of sjTREC in humans is slower than that in chickens, and the lifespan of sjTREC is less than or equal to that of T cells. Thus, we implement an uncertainty analysis

Table III. *Variables and parameters defined in the TREC model*

Variable	Definition	Value[a]	Unit	References
T_4	Total CD4⁺ T cells	4.33×10^{10}	/blood and LT	28, 29, 30
T_8	Total CD8⁺ T cells	1.80×10^{10}	/blood and LT	28, 29, 30
τ_4	Total sjTREC within CD4⁺ T cells	5.11×10^9	/blood and LT	9, 28, 29, 30
τ_8	Total sjTREC within CD8⁺ T cells	2.12×10^9	/blood and LT	9, 28, 29, 30
Parameter				
γ_1	Growth rate of CD4⁺ T cells	0.002	/day	45, 60
γ_2	Growth rate of CD8⁺ T cells	0.002	/day	45, 60
δ_1	Death rate of CD4⁺ cells	0.002	/day	45, 46, 60
δ_2	Death rate of CD8⁺ cells	0.002	/day	45, 46, 60
s_1	Half-saturation constant for CD4⁺ T cells on growth rate	10^{10}	cell	Estimated
s_2	Half-saturation constant for CD8⁺ T cells on growth rate	10^{10}	cell	Estimated
ϵ_1	Degradation rate of sjTREC within CD4⁺ T cells	0.002	/day	50, estimated
ϵ_2	Degradation rate of sjTREC within CD8⁺ T cells	0.002	/day	50, estimated
c_1	sjTREC concentration within CD4⁺ RTE	0.118	sjTREC/cell	9
c_2	sjTREC concentration within CD8⁺ RTE	0.118	sjTREC/cell	9

[a] Values for variables are initial values.

by varying the sjTREC degradation rates for CD4$^+$ and CD8$^+$ T cells. Finally, we use the value of 0.002/day as the sjTREC degradation rate.

The initial conditions (at birth) for total CD4$^+$ and CD8$^+$ T cells are 4.33×10^{10} and 1.80×10^{10}, respectively (28–30). The initial condition for total sjTREC levels within CD4$^+$ T cells is 5.109×10^9, calculated by multiplying total CD4$^+$ T cell number at birth by 0.118 sjTREC/cell (TREC concentration in RTE). Similarly, 2.124×10^9 has been calculated as the initial condition for total sjTREC level within CD8$^+$ T cells.

Once the model equations are derived and the parameter values are estimated, we then solve the system of nonlinear ordinary differential equations using an appropriate numerical method. We solve the system in two separate computational programs to ensure accuracy.

Uncertainty and sensitivity analysis

We use a Latin Hypercube Sampling scheme and PRCC (cf Ref. 39) for uncertainty and sensitivity analyses, respectively. Briefly, for the uncertainty analysis, a random sample of each of the parameters to be tested is generated from a list of parameter ranges and distributions. In our case, this sampling is done 90 times. The values in each column of the matrix generated from the sampling are randomly chosen values for a given parameter from a widely defined, evenly partitioned range of values. The sets of values in each row of the matrix are then used in 90 independent simulations. These values provide a range of results for each solution curve generated from the original parameter set. The sensitivity analysis predicts which parameter(s) have the greatest influence on the outcomes resulting from the uncertainty analysis. In our case, by comparing the values of PRCC, the relative importance of thymic and peripheral T cell events to TREC concentrations can be quantitatively evaluated.

Acknowledgments

References

1. Mackall, C. L., F. T. Hakim, and R. E. Gress. 1997. T-cell regeneration: all repertoires are not created equal. *Immunol. Today* 18:245.

2. Steinmann, G. G., B. Klaus, and H. K. Muller-Hermelink. 1985. The involution of the ageing human thymic epithelium is independent of puberty: a morphometric study. *Scand. J. Immunol.* 22:563.

3. Jamieson, B. D., D. C. Douek, S. Killian, L. E. Hultin, D. D. Scripture-Adams, J. V. Giorgi, D. Marelli, R. A. Koup, and J. A. Zack. 1999. Generation of functional thymocytes in the human adult. *Immunity* 10:569.

4. Poulin, J. F., M. N. Viswanathan, J. M. Harris, K. V. Komanduri, E. Wieder, N. Ringuette, J. M. McCune, and R. P. Sekaly. 1999. Direct evidence for thymic function in adult humans. *J. Exp. Med.* 190:479.

5. Kong, F., C. H. Chen, and M. D. Cooper. 1998. Thymic function can be accurately monitored by the level of recent T cell emigrants in the circulation. *Immunity* 8:97.

6. Berzins, S. P., R. L. Boyd, and J. F. Miller. 1998. The role of the thymus and recent thymic migrants in the maintenance of the adult peripheral lymphocyte pool. *J. Exp. Med.* 187:1839.

7. Gabor, M. J., D. I. Godfrey, and R. Scollay. 1997. Recent thymic emigrants are distinct from most medullary thymocytes. *Eur. J. Immunol.* 27:2010.

8. Hosseinzadeh, H., and I. Goldschneider. 1993. Recent thymic emigrants in the rat express a unique antigenic phenotype and undergo post-thymic maturation in peripheral lymphoid tissues. *J. Immunol.* 150:1670.

9. Douek, D. C., R. D. McFarland, P. H. Keiser, E. A. Gage, J. M. Massey, B. F. Haynes, M. A. Polis, A. T. Haase, M. B. Feinberg, J. L. Sullivan, et al. 1998. Changes in thymic function with age and during the treatment of HIV infection. *Nature* 396:690.

10. Zhang, L., S. R. Lewin, M. Markowitz, H. H. Lin, E. Skulsky, R. Karanicolas, Y. He, X. Jin, S. Tuttleton, M. Vesanen, et al. 1999. Measuring recent thymic emigrants in blood of normal and HIV-1-infected individuals before and after effective therapy. *J. Exp. Med.* 190:725.

11. Sodora, D. L., D. C. Douek, G. Silvestri, L. Montgomery, M. Rosenzweig, T. Igarashi, B. Bernacky, R. P. Johnson, M. B. Feinberg, M. A. Martin, and R. A. Koup. 2000. Quantification of thymic function by measuring T cell receptor excision circles within peripheral blood and lymphoid tissues in monkeys. *Eur. J. Immunol.* 30:1145.

12. McFarland, R. D., D. C. Douek, R. A. Koup, and L. J. Picker. 2000. Identification of a human recent thymic emigrant phenotype. *Proc. Natl. Acad. Sci. USA* 97:4215.

13. Douek, D. C., R. A. Koup, R. D. McFarland, J. L. Sullivan, and K. Luzuriaga. 2000. Effect of HIV on thymic function before and after antiretroviral therapy in children. *J. Infect. Dis.* 181:1479.

14. Douek, D. C., R. A. Vescio, M. R. Betts, J. M. Brenchley, B. J. Hill, L. Zhang, J. R. Berenson, R. H. Collins, and R. A. Koup. 2000. Assessment of thymic

15. Weinberg, K., B. R. Blazar, J. E. Wagner, E. Agura, B. J. Hill, M. Smogorzewska, R. A. Koup, M. R. Betts, R. H. Collins, and D. C. Douek. 2001. Factors affecting thymic function after allogeneic hematopoietic stem cell transplantation. *Blood* 97:1458.

16. Sempowski, G., J. Thomasch, M. Gooding, L. Hale, L. Edwards, E. Ciafaloni, D. Sanders, J. Massey, D. Douek, R. Koup, and B. Haynes. 2001. Effect of thymectomy on human peripheral blood T cell pools in myasthenia gravis. *J. Immunol.* 166:2808.

17. Hazenberg, M. D., S. A. Otto, J. W. Cohen Stuart, M. C. Verschuren, J. C. Borleffs, C. A. Boucher, R. A. Coutinho, J. M. Lange, T. F. Rinke de Wit, A. Tsegaye, et al. 2000. Increased cell division but not thymic dysfunction rapidly affects the T-cell receptor excision circle content of the naive T cell population in HIV-1 infection. *Nat. Med.* 6:1036.

18. Al-Harthi, L., G. Marchetti, C. M. Steffens, J. Poulin, R. Sekaly, and A. Landay. 2000. Detection of T cell receptor circles (TRECs) as biomarkers for de novo T cell synthesis using a quantitative polymerase chain reaction-enzyme linked immunosorbent assay (PCR-ELISA). *J. Immunol. Methods* 237:187.

19. Kraft, D. L., I. L. Weissman, and E. K. Waller. 1993. Differentiation of CD3$^-$4$^-$8$^-$ human fetal thymocytes in vivo: characterization of a CD3$^-$4$^+$8$^+$ intermediate. *J. Exp. Med.* 178:265.

20. Rosenzweig, M., D. P. Clark, and G. N. Gaulton. 1993. Selective thymocyte depletion in neonatal HIV-1 thymic infection. *AIDS* 7:1601.

21. Amadori, A., R. Zamarchi, G. De Silvestro, G. Forza, G. Cavatton, G. A. Danieli, M. Clementi, and L. Chieco-Bianchi. 1995. Genetic control of the CD4/CD8 T-cell ratio in humans. *Nat. Med.* 1:1279.

22. Haynes, B. F., M. L. Markert, G. D. Sempowski, D. D. Patel, and L. P. Hale. 2000. The role of the thymus in immune reconstitution in aging, bone marrow transplantation, and HIV-1 infection. *Annu. Rev. Immunol.* 18:529.

23. Shortman, K., M. Egerton, G. J. Spangrude, and R. Scollay. 1990. The generation and fate of thymocytes. *Semin. Immunol.* 2:3.

24. Pido-Lopez, J., N. Imami, and R. Aspinall. 2001. Both age and gender affect thymic output: more recent thymic migrants in females than males as they age. *Clin. Exp. Immunol.* 125:409.

25. Lempicki, R. A., J. A. Kovacs, M. W. Baseler, J. W. Adelsberger, R. L. Dewar, V. Natarajan, M. C. Bosche, J. A. Metcalf, R. A. Stevens, L. A. Lambert, et al. 2000. Impact of HIV-1 infection and highly active antiretroviral therapy on the kinetics of CD4$^+$ and CD8$^+$ T cell turnover in HIV-infected patients. *Proc. Natl. Acad. Sci. USA* 97:13778.

26. Wiener, D., S. Shah, J. Malone, N. Lowell, S. Lowitt, and D. T. Rowlands, Jr. 1990. Multiparametric analysis of peripheral blood in the normal pediatric population by flow cytometry. *J. Clin. Lab. Anal.* 4:175.

27. Chakrabarti, L. A., S. R. Lewin, L. Zhang, A. Gettie, A. Luckay, L. N. Martin, E. Skulsky, D. D. Ho, C. Cheng-Mayer, and P. A. Marx. 2000. Age-dependent changes in T cell homeostasis and SIV load in sooty mangabeys. *J. Med. Primatol.* 29:158.

28. Hurst, J. W. 1992. *Medicine for the Practicing Physician*, 3rd Ed. Butterworth-Heinemann, Boston, p. 128.

29. Behrman, R. E., Vaughan, V. C. 1983. *Nelson Textbook of Pediatrics*, 12th ed. W. B. Saunders, Philadelphia, p. 29 Appendix.

30. Kourtis, A. P., C. Ibegbu, A. J. Nahmias, F. K. Lee, W. S. Clark, M. K. Sawyer, and S. Nesheim. 1996. Early progression of disease in HIV-infected infants with thymus dysfunction. [Published erratum appears in 1997 *N. Engl. J. Med.* 336: 595.] *N. Engl. J. Med.* 335:1431.

31. Yanase, Y., T. Tango, K. Okumura, T. Tada, and T. Kawasaki. 1986. Lymphocyte subsets identified by monoclonal antibodies in healthy children. *Pediatr. Res.* 20:1147.

32. Mackall, C. L., L. Granger, M. A. Sheard, R. Cepeda, and R. E. Gress. 1993. T-cell regeneration after bone marrow transplantation: differential CD45 isoform expression on thymic-derived versus thymic-independent progeny. *Blood* 82:2585.

33. Mims, C. A., Dimmock, N. J., Nash, A., Stephen, J. 1997. *Mims' Pathogenesis of Infectious Disease*, 4th Ed. Academic Press, London, p. 111.

34. Hulstaert, F., I. Hannet, V. Deneys, V. Munhyeshuli, T. Reichert, M. De Bruyere, and K. Strauss. 1994. Age-related changes in human blood lymphocyte subpopulations. II. Varying kinetics of percentage and absolute count measurements. *Clin. Immunol. Immunopathol.* 70:152.

35. Rosenberg, Y. J., and G. Janossy. 1999. The importance of lymphocyte trafficking in regulating blood lymphocyte levels during HIV and SIV infections. *Semin. Immunol.* 11:139.

36. Haase, A. T. 1999. Population biology of HIV-1 infection: viral and CD4$^+$ T cell demographics and dynamics in lymphatic tissues. *Annu. Rev. Immunol.* 17:625.

37. Young, A. J. 1999. The physiology of lymphocyte migration through the single lymph node in vivo. *Semin. Immunol.* 11:73.

38. Douek, D. C., M. R. Betts, B. J. Hill, S. J. Little, R. Lempicki, J. A. Metcalf, J. Casazza, C. Yoder, J. W. Adelsberger, R. A. Stevens, et al. 2001. Evidence for increased T cell turnover and decreased thymic output in HIV infection. *J. Immunol.* 167:6663.

39. Blower, S. M., Dowlatabadi, H. 1994. Sensitivity and uncertainty analysis of complex models of disease transmission: an HIV model, as an example. *Int. Stat. Rev.* 62:229.

40. Margolick, J. B., A. D. Donnenberg, A. Munoz, L. P. Park, K. D. Bauer, J. V. Giorgi, J. Ferbas, and A. J. Saah. 1993. Changes in T and non-T lymphocyte subsets following seroconversion to HIV-1: stable CD3$^+$ and declining CD3$^-$ populations suggest regulatory responses linked to loss of CD4 lymphocytes: the Multicenter AIDS Cohort Study. *J. Acquir. Immune Defic. Syndr.* 6:153.

41. Chavan, S., B. Bennuri, M. Kharbanda, A. Chandrasekaran, S. Bakshi, and S. Pahwa. 2001. Evaluation of T cell receptor gene rearrangement excision circles after antiretroviral therapy in children infected with human immunodeficiency virus. *J. Infect. Dis. 183:1445.*

42. Su, L., H. Kaneshima, M. Bonyhadi, S. Salimi, D. Kraft, L. Rabin, and J. M. McCune. 1995. HIV-1-induced thymocyte depletion is associated with indirect cytopathogenicity and infection of progenitor cells in vivo. *Immunity 2:25.*

43. Cameron, P. U., M. G. Lowe, F. Sotzik, A. F. Coughlan, S. M. Crowe, and K. Shortman. 1996. The interaction of macrophage and non-macrophage tropic isolates of HIV-1 with thymic and tonsillar dendritic cells in vitro. *J. Exp. Med. 183:1851.*

44. Braun, J., H. Valentin, M. T. Nugeyre, H. Ohayon, P. Gounon, and F. Barre-Sinoussi. 1996. Productive and persistent infection of human thymic epithelial cells in vitro with HIV-1. *Virology 225:413.*

45. Hellerstein, M., M. B. Hanley, D. Cesar, S. Siler, C. Papageorgopoulos, E. Wieder, D. Schmidt, R. Hoh, R. Neese, D. Macallan, S. Deeks, and J. M. McCune. 1999. Directly measured kinetics of circulating T lymphocytes in normal and HIV-1-infected humans. *Nat. Med. 5:83.*

46. McCune, J. M., M. B. Hanley, D. Cesar, R. Halvorsen, R. Hoh, D. Schmidt, E. Wieder, S. Deeks, S. Siler, R. Neese, and M. Hellerstein. 2000. Factors influencing T-cell turnover in HIV-1-seropositive patients. *J. Clin. Invest. 105:R1.*

47. Chakrabarti, L. A., S. R. Lewin, L. Zhang, A. Gettie, A. Luckay, L. N. Martin, E. Skulsky, D. D. Ho, C. Cheng-Mayer, and P. A. Marx. 2000. Normal T-cell turnover in sooty mangabeys harboring active simian immunodeficiency virus infection. *J. Virol. 74:1209.*

48. Steffens, C. M., L. Al-Harthi, S. Shott, R. Yogev, and A. Landay. 2000. Evaluation of thymopoiesis using T cell receptor excision circles (TRECs): differential correlation between adult and pediatric TRECs and naive phenotypes. *Clin. Immunol. 97:95.*

49. Hassan, J., and D. J. Reen. 2001. Human recent thymic emigrants: identification, expansion, and survival characteristics. *J. Immunol. 167:1970.*

50. Kong, F. K., C. L. Chen, A. Six, R. D. Hockett, and M. D. Cooper. 1999. T cell receptor gene deletion circles identify recent thymic emigrants in the peripheral T cell pool. *Proc. Natl. Acad. Sci. USA 96:1536.*

51. Luettig, B., A. Sponholz, C. Heerwagen, U. Bode, and J. Westermann. 2001. Recent thymic emigrants (CD4$^+$) continuously migrate through lymphoid organs: within the tissue they alter surface molecule expression. *Scand. J. Immunol. 53:563.*

52. Mehr, R., and A. S. Perelson. 1997. Blind T-cell homeostasis and the CD4/CD8 ratio in the thymus and peripheral blood. *J. Acquir. Immune Defic. Syndr. Hum. Retrovirol. 14:387.*

53. Ritter, M. A., and D. B. Palmer. 1999. The human thymic microenvironment: new approaches to functional analysis. *Semin. Immunol. 11:13.*

54. George, A. J., and M. A. Ritter. 1996. Thymic involution with ageing: obsolescence or good housekeeping? *Immunol. Today 17:267.*

55. Kirschner, D. E., R. Mehr, and A. S. Perelson. 1998. Role of the thymus in pediatric HIV-1 infection. *J. Acquir. Immune Defic. Syndr. Hum. Retrovirol. 18:95.*

56. Heitger, A., H. Greinix, C. Mannhalter, D. Mayerl, H. Kern, J. Eder, F. M. Fink, D. Niederwieser, and E. R. Panzer-Grumayer. 2000. Requirement of residual thymus to restore normal T-cell subsets after human allogeneic bone marrow transplantation. *Transplantation 69:2366.*

57. Roux, E., F. Dumont-Girard, M. Starobinski, C. A. Siegrist, C. Helg, B. Chapuis, and E. Roosnek. 2000. Recovery of immune reactivity after T-cell-depleted bone marrow transplantation depends on thymic activity. *Blood 96:2299.*

58. Egerton, M., R. Scollay, and K. Shortman. 1990. Kinetics of mature T-cell development in the thymus. *Proc. Natl. Acad. Sci. USA 87:2579.*

59. Haynes, B. F., and L. P. Hale. 1998. The human thymus. A chimeric organ comprised of central and peripheral lymphoid components [Corrected and republished in *Immunol. Res. 1998;18:175*]. *Immunol. Res. 18:61.*

60. McLean, A. R., and C. A. Michie. 1995. In vivo estimates of division and death rates of human T lymphocytes. *Proc. Natl. Acad. Sci. USA 92:3707.*